Pulsating Flame Spread Over Liquids

A. ITO,* K. SAITO** and C. J. CREMERS
Combustion and Fire Research Laboratory
Dept. of Mechanical Engineering
University of Kentucky
Lexington, KY 40506

ABSTRACT

This study was undertaken as an effort to improve our understanding of the mechanisms of pulsating flame spread over liquids. A holographic interferometry technique was applied to obtain a time series of simultaneous temperature profiles in gas and liquid phases for pulsating spread over propanol. Liquid motion at the free liquid surface was visualized using a particle–track technique and recorded with a high speed, high resolution video–camera from which pulsation frequency and flame behavior were analyzed. Our experimental results support the hypothesis that the primary control mechanism of pulsating spread is subsurface–liquid flow, while the effect of gas–phase convection is secondary even though it governs flame pulsation. To evaluate this interpretation, two dimensional incompressible flow equations were numerically solved and fluid dynamic structure was simulated as a function of fuel–layer thickness. The calculation results explain the present and NASA's experimental results and support our proposed mechanism of pulsating spread.

Key words: pulsating flame spread; holographic interferometry; flammability of liquids

INTRODUCTION

Flame spread over liquids is our current focus in both fundamental research into its mechanisms and applied research into its role in fires involving liquid fuels. Kinbara [1] conducted pioneer studies in Japan in the period 1930 through 1942. Recently, Ross [2] provided a review on the current progress of research on flame spread over liquids addressing several unsolved problems that need to be studied. One of them is the mechanism of pulsating flame spread, the topic of this paper.

This is a continuation of our previous study on flame spread over liquids [3]. In that study we applied holographic interferometry (HI) to obtain a detailed and instantaneous temperature distribution in the liquid phase near the fuel surface. In each of methanol, ethanol and propanol we found two different circulations in both the uniform spread region, where the flame spreads uniformly, and the pulsating spread region, where pulsating flame spread occurs. We think that the formation of the double circulation zone is due to two different mechanisms, one is a thin layer of flow driven by

* Present Address of A. Ito: Department of Production System Engineering, Oita University, Oita 870–11, Japan.
** Corresponding author: K. Saito, Tel. (606) 257–1685/Fax. (606) 257–3304.

surface tension and the other is a circulating gravity driven flow. To confirm this, however, flame–spread tests under microgravity or a theoretical investigation might be helpful. In reference to our study, Ross and Sotos [4], and Miller and Ross [5] conducted a series of flame–spread tests over shallow and deep pool alcohols using NASA's drop tower facility. They showed that when the atmospheric nitrogen was replaced with argon, the expected lowering of the flash point resulted because of the different thermal properties of the diluent. Interestingly, pulsating spread did not occur in either shallow or deep pool experiments [4], instead the flame was extinguished indicating the importance of the gas–phase–buoyancy effect on the pulsating mechanism. Fluid dynamic structures of flame induced liquid flow were numerically studied by Di Blasi et al. [6] and those of flame induced gas flow were numerically studied by Schiller and Sirignano [7]. Di Blasi et al. found that in the pulsating flame spread a large subsurface circulation split into smaller cells, however the role of these cells in the flame pulsation was left unknown. In the gas phase just ahead of the flame's leading edge, Schiller and Sirignano predicted the existence of a very small circulation which they interpreted as an important mechanism in flame spread; therefore, they claimed that the spread is under gas–phase control. Both predictions are certainly interesting, yet they need to be confirmed by experiments because both models include assumptions. In addition, note that when detailed comparison is made between theory and experiment, extreme care should be taken because all experiments involve some uncontrollable parameters, which can be best chosen by the experimenter's experience and intuition rather than theory [8–10]. This subtle and often unwritten part of experimental technique sometimes causes a significant difference in experimental data.

In this paper we attempt to explain the mechanisms of pulsating spread through newly obtained HI temperature maps for both gas and liquid phases and particle–track flow–visualization at the free liquid surface. Through HI measurements, we found that the pulsating spread consisted of a steady component, where the liquid–surface temperature close to the flame leading edge is below the closed cup flash–point; and a rapid accelerating component, where the liquid–surface temperature exceeds the flash point [3]. Therefore, it is reasonable to conclude in agreement with Glassman and Dryer [11] that pulsating spread is the result of the alternative appearance of gas–phase spread and liquid–phase spread. This interpretation is also consistent with experimental results obtained by other researchers [12–14]. However, an essential question still remains: whether the pulsating spread is controlled by the gas phase or liquid phase or is it a combination of both? Our experimental results and theoretical evaluation seem to support that it is both; liquid flow is the principal driving force for pulsating spread and gas–phase structure, which is responsible for the flame pulsation, is closely linked with it.

EXPERIMENTAL METHODS

The experimental apparatus (shown in Figure 1) and the optical system for HI used for this study are the same as those used in previous flame spread study [3]. The two long sides of the fuel tray were made of Pyrex of 0.1 cm thickness. Propanol was used as fuel, since it provides a common database for us to allow comparison of our data to NASA's microgravity data [4,5] and our previous experiments [3]. The fuel was uniformly ignited at one end by a small pilot flame. To measure the spread rate of the subsurface liquid flow, we sprinkled 5 μm–diameter aluminum–particles onto the liquid surface. That the aluminum particles float on the liquid surface and follow closely the direction of the subsurface–liquid flow was confirmed by comparing a time series of simultaneous interferograms for both gas and liquid phases with the video taped behavior of the aluminum–particles.

A He–Ne laser of 5–mW power and 632.8–nm wavelength was used as the beam source. The main beam was split into object and reference components. The test section was placed in the object beam. A facility was created to develop in situ an interferogram plate that was held in its original position during the experiments. An

interferogram with a clear separation of fringes is important to obtain accurate temperatures. We used several different tray widths and found that a tray with width between 1 and 4 cm best satisfies the requirement of uniform and short path length through the liquid and Pyrex. This also satisfies two dimensionality of temperature profiles in the liquid phase. To check the dependence of pulsating spread on the tray width and to obtain the maximum resolution for HI measurement for gas and liquids, both 1 and 4 cm wide trays were used. A fuel layer of 2–cm thickness was experimentally shown to satisfy the deep pool condition [3,15] and was used for all HI and aluminum–trace measurements. Assuming the laser beam, which is in the z direction (Figure 1) and normal to the tray side wall, is straight and the temperature variation along it is negligible, the relationship between the fringe number and temperature can be obtained as previously described in detail [3].

For the liquid phase, the reference temperature for the interferogram was obtained by a copper–constantan thermocouple of 50–μm diameter and the spatial resolution for the interferogram was determined to be 30 μm. Also, an error estimate was made of the accuracy of our interferogram considering temperature dependence of the thermo–optic coefficient, refraction of light, and temperature distribution in liquid along the light beam. The estimated total maximum error was found to be less than 3% of the temperature at the center of the liquid [3]. Thus, our holographic interferometry system is accurate enough to study the detailed temperature structure in the liquid phase. However, less accuracy is expected for gas–phase interferograms due to the curved flame–front line and three–dimensional structure of the flame shape. Therefore, gas–phase temperature–profiles were not deduced from interferograms, instead the latter were used to determine the thermal boundary structure of the gas–phase.

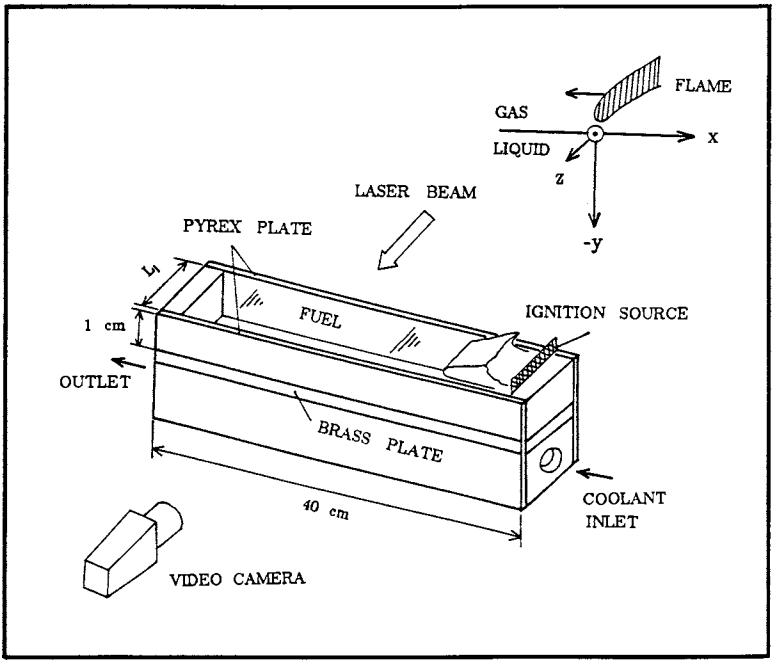

Figure 1 Schematic diagram of flame spread apparatus.

RESULTS AND DISCUSSION

Interferogram and Particle–Track Results

Two different series of interferograms for propanol (flash point = 25 deg. C) for the pulsating region at a liquid temperature of 12.1 deg. C with the 4 cm wide tray and 13.5 deg. C with the 1 cm wide tray are respectively shown in Figures 2 and 3. One series contains six photographs obtained in time intervals of 0.2 s, while the other contains four photographs obtained in time intervals of 0.25 s. Two different types of flame are identified from the interferograms (Figures 2b–2e) and color–video tapes taken from the side. One is the main flame (MF) whose leading edge is opaque blue, and the other is an intermittent finger flame (FF), previously observed by Burgone et al. [12] and Glassman et al. [16], whose color is pale blue and which is quite unstable. Although the two–flame structure exists for both tray widths (which was confirmed by visual observation), it is not clearly identifiable from the interferograms taken when using the 1 cm wide tray due to its short path length and larger heat loss to the side wall. However, Figure 3 interferograms clearly show the process of pulsating spread which consists of a rapid acceleration of the gas–phase spread driven by the subsurface–liquid flow (a–b) and a momentary stagnation of both liquid–phase and gas–phase spread (c–d).

The time history of the location of the flame leading edge and the direction of the subsurface–liquid flow for the pulsating spread region were recorded. The location of the flame leading edge was determined from the time series of interferograms and color–video tapes; and the location of the direction of the subsurface–liquid flow was determined from the time series of interferograms and the video taped trace of aluminum particles floating on the liquid surface. Based on those measurements, the spread rates of the leading edges of the main flame V_m and finger flame V_f, and subsurface–liquid–convection current V_s are plotted in Figure 4 as a function of time (the times taken for the six different interferograms shown in Figures 2a–2f are indicated in Figure 4). It can be seen from Figure 4 that the V_s for steps (a) through (e) are approximately in a steady state condition with nearly the same spread rate (3.2 ± 0.5 cm/s). By contrast, during the same periods both main and finger flames showed rapid acceleration and deceleration modes. In step (e), the starting point of the cycle of pulsating spread and the location of the head of liquid flow and flame leading edge are at approximately the same position. For steps (e)–(f) V_s, V_m and V_f are all in the acceleration mode; the acceleration rate of V_s is highest, V_f is second and V_m is lowest proving that the subsurface–liquid flow spreads first, then the gas–phase spread follows. In the next step, the liquid flow slows down (step (a)) due to insufficient heat from the flame, which lets the flame leading edge reach the head of the subsurface–liquid flow where it slows down and stops momentarily; then a new circulation zone of subsurface–liquid flow is formed in front of the location of the old circulation zone (step (e)) completing the pulsating cycle.

Interferograms (for both liquid phase and gas phase) and video taped flame and aluminum–particle behaviors confirm that the front of the subsurface–liquid flow is always ahead of the flame leading edge and the distance between these changes in accordance with the flame pulsation, indicating that the spread is controlled by the subsurface–liquid flow from which the gas–phase (pulsating) results. To further confirm this, time averaged gas– and liquid–phase spread–rates were calculated from the HI and aluminum–trace data over several different cycles of flame–pulsation periods. It was found that the two spread rates were identical supporting the above interpretation.

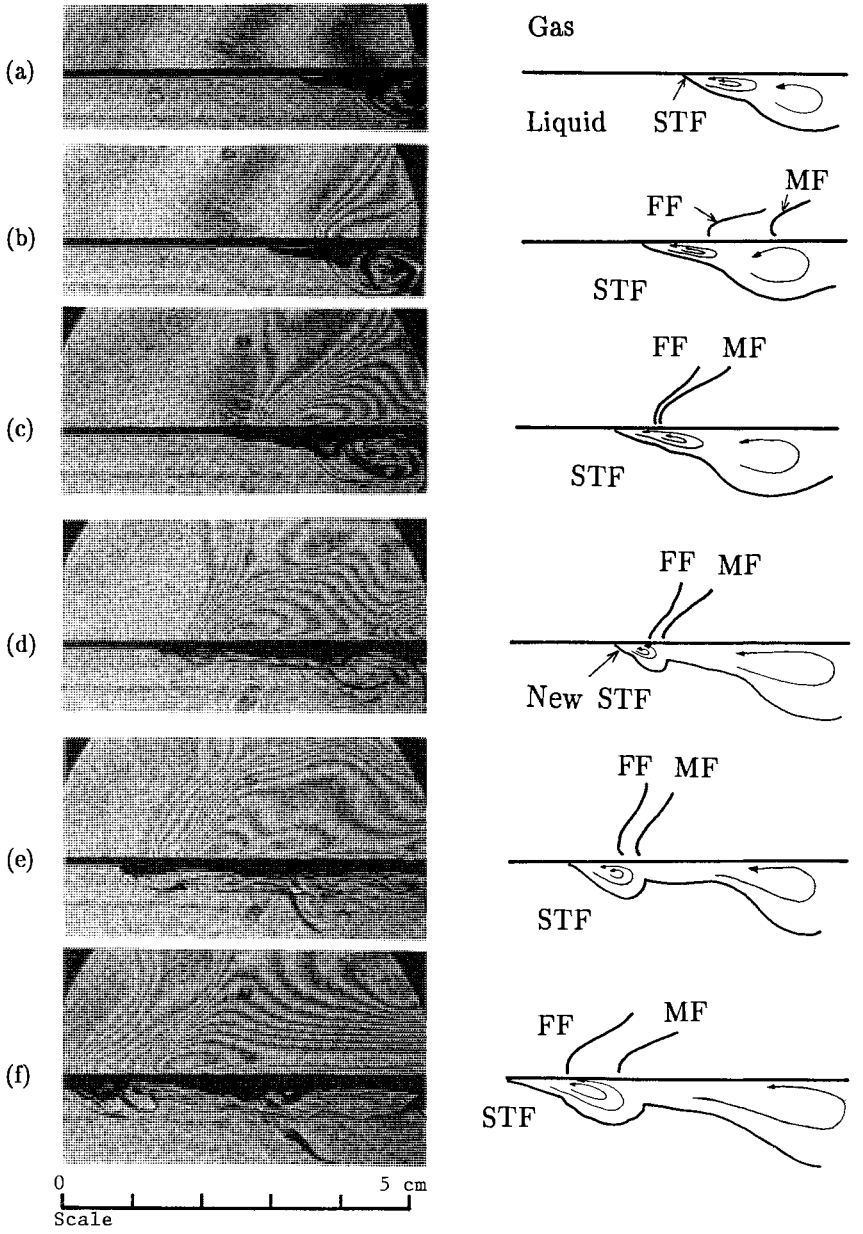

FIGURE 2 Six different interferograms (a–f) obtained in 0.2 s from (a) to (f) and the thermal boundary location of finger flame (FF) and of main flame (MF) for propanol with Initial liquid temperature, 12.1 °C and tray width 4 cm.

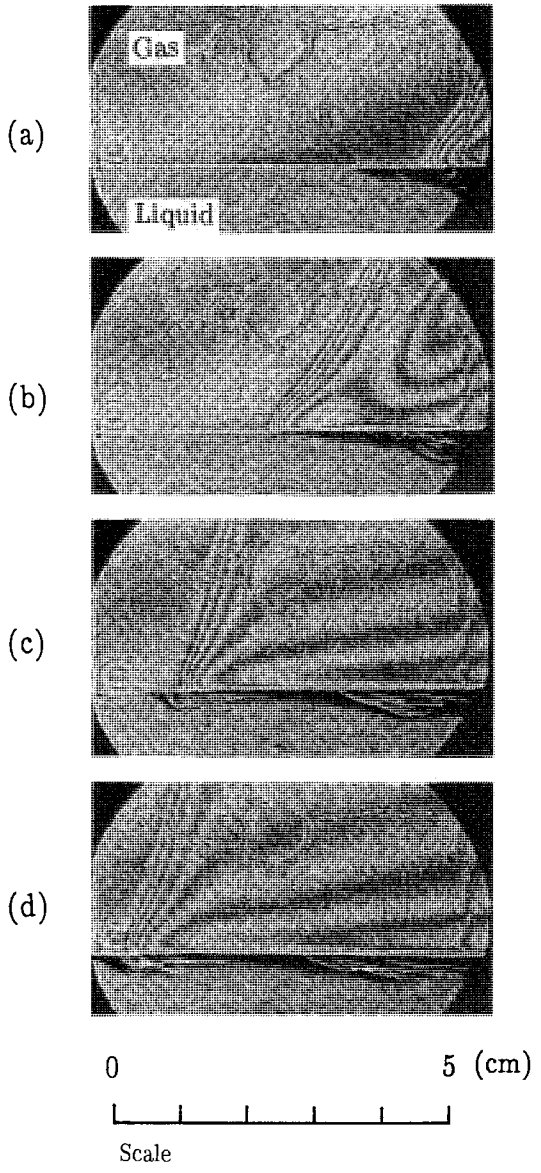

FIGURE 3 Four different interferograms (a–d) obtained in 0.3 s from (a) to (d) for propanol with initial liquid temperature, 13.5 deg.C and tray width = 1 cm.

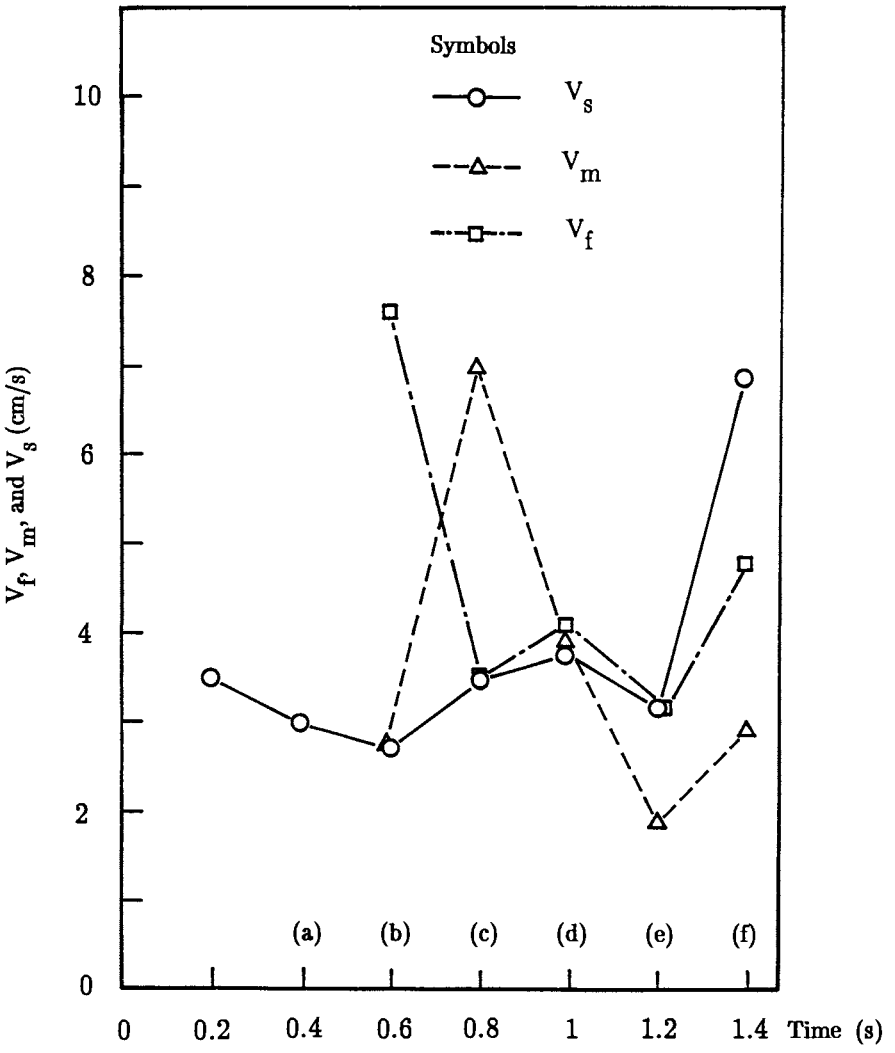

FIGURE 4 Spread rate of finger flame (V_f), of main flame (V_m) and of subsurface–liquid flow (V_s) as a function of time. The gas–phase spread rate was determined from the video tape and interferograms; liquid–phase spread rate was determined from the trace of video–taped aluminum–particles.

Theoretical Considerations

To theoretically evaluate the role of the liquid phase in pulsating spread, we developed a two–dimensional line–heat source (stationary flame) model using the following conservation laws for mass, x–momentum, y–momentum and energy, respectively:

$$\partial u/\partial x + \partial v/\partial y = 0, \tag{1}$$

$$\partial u/\partial t + u\partial u/\partial x + v\partial u/\partial y = -(1/\rho)\partial p/\partial x + \nu\partial^2 u/\partial x^2 + \nu\partial^2 u/\partial y^2, \tag{2}$$

$$\partial v/\partial t + u\partial v/\partial x + v\partial v/\partial y = -(1/\rho)\partial p/\partial y + \nu\partial^2 v/\partial x^2 + \nu\partial^2 v/\partial y^2 - g\beta(T - T_0), \tag{3}$$

and

$$\partial T/\partial t + u\partial T/\partial x + v\partial T/\partial y = \alpha\partial^2 T/\partial x^2 + \alpha\partial^2 T/\partial y^2. \tag{4}$$

Here u = velocity component in the x direction, v = velocity component in the y direction, x = horizontal coordinate, y = vertical coordinate, p = pressure, T = liquid temperature, ρ = density of liquid, ν = kinematic viscosity of liquid, g = acceleration due to gravity, β = thermal expansion coefficient, and α = thermal diffusivity.

Heat flux at the fuel surface is given as $q = -k(\partial T/\partial y)$, where k is the thermal conductivity of liquid. Tangential and normal stress balances at the surface can be respectively written as follows,

$$\partial u/\partial y + \partial u/\partial x + 2\partial h/\partial x(\partial v/\partial y - \partial u/\partial x) = (1/\mu)(d\sigma/dT)(\partial T/\partial x) \tag{5}$$

$$-p + 2\mu[\partial v/\partial y - \partial h/\partial x(\partial u/\partial y + \partial v/\partial x)] = \sigma(\partial^2 h/\partial x^2) \tag{6}$$

Here h = fuel depth, μ = liquid viscosity, and σ = surface–tension force. Governing equations (1) through (4) were numerically solved using a finite difference method [17]. The model calculation shows that the number of closed loop circulations in the fuel layer increase with decreasing fuel–layer thickness (calculation results for fuel depth, 1.3 and 5.1 mm are shown in Figure 5), indicating that a thin and long circulation structure is physically unstable, and therefore it converts to several smaller round circulations which are relatively stable and likely to transfer the convective heat more effectively. Di Blasi [6] also numerically showed that when the flame pulsation occurred, a large circulation periodically decays into smaller ones. The alternative appearance of the large and small circulation is likely related to flame pulsation. Our recent HI data [18] confirmed that the frequencies of the flame pulsation and the alternation of the large and small eddies agree very well. The liquid phase was heated by an infrared line heater and its liquid–circulation structure was visualized by 5–μm–aluminum particles for both 1.3 mm and 5.1 mm deep water; those results clearly support the simulation results [17].

NASA conducted a series of flame–spread tests under normal gravity using a 2 cm wide tray for propanol with three different fuel thicknesses (2, 5 and 10 mm). Their results [5] demonstrated the dependence of pulsating frequency on the fuel thickness. For 2 mm deep fuel the pulsation frequency was approximately 2 Hz, for 5 mm deep fuel it was 1.2 Hz and for 10 mm deep fuel it was 1 Hz. Those experimental results compare well with the numerical simulation results that demonstrate the change of circulation structure in the liquid phase. A large single circulation in the 5 mm deep fuel likely causes a relatively long pulsation length over which the flame pulsates with a relatively low frequency, while small multiple circulations in the 2 mm deep fuel cause a relatively short pulsation length over which the flame would pulsate with a relatively high

frequency.

Previously we studied flame spread over wood [19] and observed a periodic flame propagation similar to the flame pulsation over liquids. Our report [19] states: "When external radiant heat is set up between 0.5 W/cm^2 and 0.7 W/cm^2, the pilot initiated a small yellow flame that soon died, then ignited a transient blue flame that traveled to the edge of the sample. Five or six periodical repetitions of this blue flame initiation and propagation were observed before the external heat flux had increased the char layer thickness to such an extent that gasification rates were insufficient to provide concentrations of gaseous combustibles high enough for reignition. This general type of periodic premixed–flame propagation is not indicative of sustained spread." This observation suggests that the triggering mechanism of the flame pulsation may exist in the gas phase.

Why does Flame Extinction Occur under Microgravity ?

Through carefully designed drop tower experiments, Ross and Miller showed [5] that the pulsating spread did not occur under microgravity, instead the flame was extinguished. To understand why, we carefully reviewed the video taped interferograms of pulsating spread under normal gravity. We noticed that to realize the pulsating spread, the gas–phase spread must follow the subsurface–liquid flow which yields a rapid acceleration (the resulted maximum spread rate is 7 cm/s as shown in Figure 4) right after the step (e) in Figures 2 and 4. Under normal gravity, this can be accomplished with the help of buoyancy induced flow which carries away combustion products and supplies fresh air to the flame leading edge as suggested by Bhattacharjee and Altenkirch [20] and Miller and Ross [5]. However, under microgravity the expected slower gas–phase spread [20,21] may not be able to follow the relatively fast liquid flow causing a sudden separation of the flame leading edge from the head of the subsurface–liquid flow. If this occurred under a poorly mixed fuel–air environment, chemical reactions necessary to sustain combustion may not occur, therefore possibly leading to extinction of the flame.

To quantify this idea, we compared response time in the liquid phase to mixing time in the gas phase for both normal and microgravity conditions. The response time (t_r) and the mixing time (t_x) are respectively defined by $t_r = L/V_s$ and $t_x = L/(V_{diff} + V_{conv})$. Here L is the characteristic length in the x–direction, V_{diff} is the ratio of molecular diffusivity to L, and V_{conv} is the velocity component normal to the flame sheet. The characteristic length was determined to be 1 cm from the interferograms obtained for gas and liquid phases (see Figure 6), spread–rate of the liquid phase was obtained from the interferograms (see Figure 4), and the diffusion rate was on the order of 1 cm/s.

To determine the convection rate for the spreading flame with pulsation, a direct quantitative measurement is very difficult although it may be possible. Therefore, we applied our velocity–profile data, which were obtained for the flame base of a propanol pool fire of 6 cm diameter using a phase–doppler particle–analyzer [21], to the spreading flame. For the spreading flame, locations of the thermal boundary and the leading flame edge were determined from both interferograms and color photographs, while for the pool fire the location of the leading flame edge was determined from color photographs. Then, a matching of the leading flame–edge location was made for the two flames and the flame–spread rate was added to the measured horizontal velocity component (Figure 6). From Figure 6, $V_{conv} \cong 20$ cm/s was obtained for the vicinity of the leading flame edge whose heat balance is crucial to determining flame–spread rate. Finally using the above values, we obtained $t_r/t_x = 2.6$ for the pulsating spread region under normal gravity, while for the same liquid temperature under microgravity, $t_r/t_x = 0.5$ due to

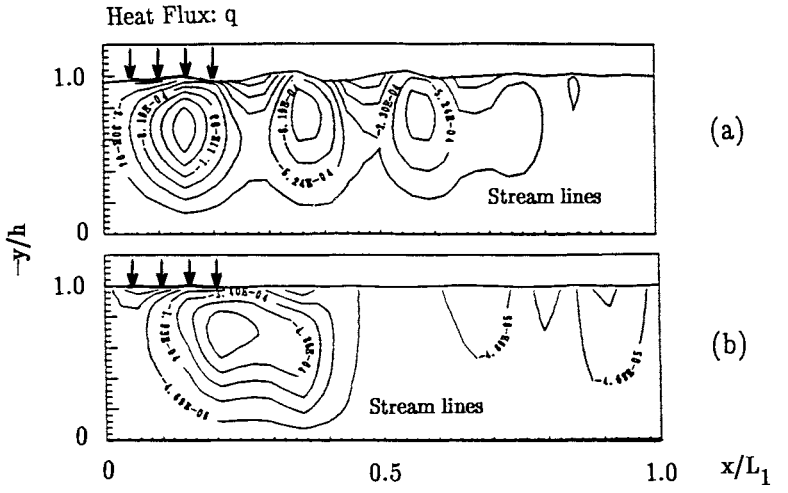

FIGURE 5 Numerical results for a water layer (a) with 1.3–mm depth and 2.6 s after the exposure of a 276–W line–heater, and (b) with 5.1–mm depth and 2.0 s after the exposure of a 276–W line–heater (for details, see [16]).

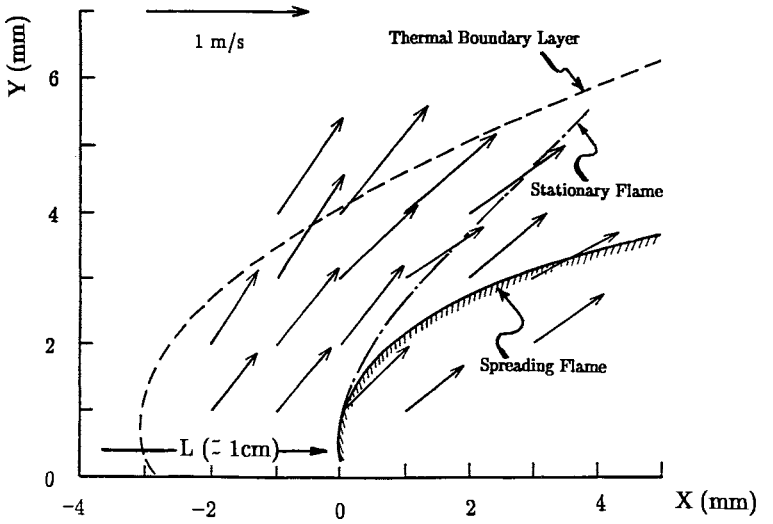

FIGURE 6 Velocity vectors for a spreading flame over propanol near the flame leading edge. The vectors were obtained by adding spread rate to the measured velocity vectors for a propanol–pool fire of 6 cm diameter using a two–component–phase–doppler particle–analyzer [20].

the absence of gas–phase convection. The estimation was extended to the uniform spread region: $t_r/t_x = 2.1$ was obtained for normal gravity, $t_r/t_x = 1.1$ was obtained for microgravity, and both cases resulted in the same spread rate suggesting gravity may have no role in this region. That under microgravity the smaller t_r/t_x (0.5) for pulsating spread and the larger t_r/t_x (1.1) for uniform spread were obtained is due to the fact that for pulsating spread, the liquid–phase spread–rate is twice as high as that of the gas–phase spread–rate at the beginning of the pulsation cycle (Figures 4e–4f). However, for uniform spread the liquid–phase spread and gas–phase spread are approximately the same. This suggests that under microgravity if the difference between the liquid–phase spread–rate and the gas–phase spread–rate exceeds the diffusion rate, the flame is unable to spread and eventually reaches extinction. The above estimation seems to indicate the existence of a critical (t_r/t_x) value, a number between 0.5 and 1.1, above which the flame is able to spread and below which flame extinction occurs. To further develop the above argument, however, an extensive series of experiments or rigorous theoretical investigation is needed.

SUMMARY AND CONCLUSIONS

(1). The holographic interferometry technique was applied to obtain the detailed temperature structure of both liquid and gas phases for a pulsating flame spread over propanol. Small aluminum particles were sprinkled as a tracer onto the liquid surface to visualize the liquid flow and their motion was recorded with a high–speed, high–resolution video camera. From this, the pulsation frequency and relative distance between the direction of the subsurface–liquid flow and flame leading edge were determined. Experiments indicate that the pulsating spread rate is governed by the subsurface–liquid flow, and gas–phase spread is secondary.

(2). To support the above interpretation, we numerically solved the two–dimensional, incompressible flow equations. These results showed the significant dependence of flow structure on fuel thickness. This simulation result explains our and NASA's experimental data consistently and therefore supports our interpretation of the mechanism of pulsating spread over liquids.

(3). The extinction condition for flame spread over liquids was discussed with the idea of using a nondimensional time defined by the ratio of mixing time for the gas phase to the response time for the liquid phase. This appears to be consistent with experimental results under normal and microgravity conditions. However, further experimental or theoretical studies are needed to confirm the proposed extinction criterion.

ACKNOWLEDGEMENTS

This work was supported from NASA under Grant (NAG3–1296) and from the Center for Robotics and Manufacturing Systems, University of Kentucky under a matching grant. We thank H. Ross and F. Miller for providing us with their experimental data and for stimulating technical discussions, and M. Mawatari for his assistance in the HI measurements.

REFERENCES

1. Kinbara, T., Bulletin of Institute of Physical Chemistry Research Japan, 9: 561–570 (1930); 10: 37–51 (1931); 11: 104–119 and 1191–1200 (1932); 15: 871–885 and 1090–1094 (1936); and 21: 95–110 (1942).

2. Ross, H.D., Progress in Energy and Combustion Sciences, 1994 (to appear).

3. Ito, A, Masuda, D, and Saito, K., Combustion and Flame, 83: 375–389 (1991).

4. Ross, H.D. and Sotos, R.G., Twenty–third Symposium (International) on Combustion, The Combustion Institute, 1990, pp. 1649–1655.

5. Miller, F.J. and Ross, H.D., Twenty–fourth Symposium (International) on Combustion, The Combustion Institute, 1992, pp. 1703–1711.

6. Di Blash, C., Crescitelli, S., and Russo, G., Twenty–third Symposium (International) on Combustion, The Combustion Institute, 1990, pp. 1669–1675.

7. Schiller, D.N. and Sirignano, W.A., Presented at the Western States Section of the Combustion Institute Meeting, October, 1991, Los Angeles, CA.

8. Wilson, E.B., Jr., An Introduction to Scientific Research, McGraw–Hill, New York, NY, 1956, Chap. 4.

9. Hirano, T., and Saito, K., Progress in Energy and Combustion Sciences, 1994 (submitted).

10. Saito, K., "Kufu: Western Mode of Logical Thinking vs. Eastern Mode of Intuitive Cognition," Department of Mechanical Engineering Report, The University of Kentucky, Lexington, KY 40506.

11. Glassman, I. and Dryer, F.L., Fire Safety Journal, 3: 123–138 (1980).

12. Burgoyne, J.H. Roberts, A.F., and Quinton, P.G., Proc. the Royal Society, A 308: 39–53 (1968).

13. Burgone, J.H. and Roberts, A.F., Proc. the Royal Society, A 308, 69–79 (1968).

14. Mackinven, R., Hansel, J. and Glassman, I., Combustion Science and Technology, 9: 293–306 (1970).

15. Williams, F.A., Combustion Theory, Second Edition, Benjamin/Cummings, Menlo Park, CA, 1985, Chap. 12.

16. Glassman, I., Hansel, J. and Eklund, T., Combustion and Flame, 13: 199–101 (1969).

17. Fukano, T., Choudhury, S.K. and Ito, A., "Thermocapillary Flow in Thin Liquid Layers," Memoir of Faculty of Engineering, Kyushu University, Kyushu, Japan, Vol.50, June 1990, pp. 75–105.

18. Ito, A, and Saito, K., unpublished data, 1994.

19. Saito, K., Williams, F.A., Wichman, I.S., and Quintiere, J.G., J. Heat Transfer, 111: 438–445 (1989).

20. Bhattacharjee, S. and Altenkirch, R.A., Twenty–third Symposium (International) on Combustion, The Combustion Institute, 1990, pp. 1627–1633.

21. Venkatesh, S, Ito, A, and Saito, K., "Anchoring Mechanism of Liquid Pool Fires," Department of Mechanical Engineering Report, The University of Kentucky, Lexington, KY 40506.